Agriculture, Environment & Society (2022) Volume 2, Issue 1, P. 31-39

Agriculture, Environment & Society

Journal homepage: www.aes.uoz.ac.ir

Evaluation of some engineering properties of green almond for mechanical harvesting

Hajarsadat Seyedalibeyk Lavasani [a], Jalal Baradaran Motie [*b]

[a] M.Sc student of Biosystems Engineering, Ferdowsi University of Mashhad, Mashhad, Iran
[b] Department of Biosystems Engineering, Ferdowsi University of Mashhad, Mashhad, Iran

ARTICLE INFO

Article history:
Received: 23 February 2022
Accepted: 27 April 2022
Available online: 15 May 2022

Keywords:
Almond
Compression test
Mass modelling
Mechanical properties
Physical properties

ABSTRACT

Green almonds are a seasonal treat, and mechanical harvesting of green almonds has the potential to increase their consumption while also introducing a new method of reducing almond processing costs and residue. The purpose of this study was to investigate the physical properties and mechanical behavior of green almonds of the Sahand variety. The physical properties measured were length, width, thickness, arithmetic and geometric mean diameters, which averaged 29.73, 20.23, 15.02, 21.66, and 20.81 mm, respectively. Additionally, the surface and projected areas, aspect ratio, sphericity, mass, volume, true density, and porosity were determined to be 1366.77 mm2, 473.59 mm2, 0.68, 0.70, 4.14 g, 3.78 cm3, 1.10 g/cm3, and 0.44. Almost all of the physical properties of green almonds studied were found to be correlated. Green almonds had a static friction coefficient of 0.519, 0.441, and 0.523 on MDF, galvanized iron, and rubber, respectively, and the static friction coefficients on MDF and rubber were not significantly different at the 1% confidence level. A uniaxial compression test was used to investigate the mechanical behavior of green almonds under compression. The tests were conducted in three directions (X, Y, and Z, which correspond to the length, width, and thickness of green almonds, respectively) and at three speeds (10, 15, and 20 mm/min). The results indicated that only direction had a significant effect on the mechanical test results and that green almonds can withstand greater deformation along their length before rapture.

Highlights

- This research looked into the physical and mechanical properties of Sahand green almonds.
- The average length, width, thickness, arithmetic and geometric mean diameters were 29.73, 20.23, 15.02, 21.66, and 20.81 mm.
- The surface and projected areas, aspect ratio, sphericity, mass, volume, true density, and porosity were determined to be 1366.77 mm2, 473.59 mm2, 0.68, 0.70, 4.14 g, 3.78 cm3, 1.10 g/cm3, and 0.44.
- Green almonds had static friction coefficients of 0.519, 0.441, and 0.523 on MDF, galvanized iron, and rubber, respectively.

1. Introduction

Over a period of ten years, almond production around the world has increased by one million tons and has almost reached 3.5 million tons in 2019 (FAOSTAT, 2021). The almond kernel consumed by humans only accounts for 15% of the mature almond fruit weight, while more than half of its total fresh weight is its hull (Prgomet et al., 2017). Therefore, managing and reducing almond residue, including its hull, is crucial. While almond by-products are used for energy production and as livestock feed, some novel applications have been discovered and utilized. For example, almond residue is a source of biomass (Akubude and Nwaigwe, 2016; Huang and Lapsley, 2019) and hydrothermal treatment of almond hulls can create biofuel (Remón et al., 2021). The green outer hull of almond is efficient for removing cobalt (Ahmadpour et al., 2009) and chromium(VI) (Nasseh et al., 2017) from contaminated water. It is also used as livestock feed (DePeters et al., 2020; Gupta et al.,

* Corresponding author
Email: j.baradaran@um.ac.ir (J. Baradaran)
http://dx.doi.org/10.22034/aes.2022.331121.1024

2020). Almond shell can be used in particleboard mixture (Pirayesh and Khazaeian, 2012; Ferrandez-Villena et al., 2019), polypropylene (Essabir et al., 2013; Appah et al., 2019), and polybutylene succinate (PBS) composite (Liminana et al., 2018). Deionization systems can use activated carbon made from an almond shell as an electrode material (Maniscalco et al., 2020).

Extensive research has been done on the importance and characteristics of almonds (Esfahlan et al., 2010; Özcan et al., 2011) and the physical properties and mechanical behavior of mature almond kernels and shells (Aydin, 2003; Ledbetter and Palmquist, 2006; Aktas et al., 2007; Rasouli et al., 2010; Demir et al., 2019; Sakar et al., 2019; Gradziel, 2020; Zahedi et al., 2020)(. It should be noted that the physical properties of fresh products can be used for classification purposes (Baradaran Motie et al., 2014). Moreover, new systems have been developed for estimating and predicting the physical properties of mature almonds based on variety (Eski et al., 2018) and shell features (Miraei Ashtiani et al., 2020). The Green almond is an unripe form of almond, which is harvested from almond trees before maturing (when it is harvested for its kernel) and is consumed whole in spring. Although green almonds are consumed in many countries around the world and are even sold online, no official statistics or data were found on green almond production. Green almonds are one of the most popular snacks in the middle east and some other parts of the world, which are consumed entirely with their hull and shell, so that by expanding their consumption. It can increase the profit of producers (due to higher selling prices) and also reduce the production of almond waste. However, data on green almonds is relatively scarce (Murathan et al., 2020). To our knowledge, no research has been done on the physical properties of green almonds.

This study aims to determine the physical properties of green almonds of the Sahand variety around 70 days after anthesis (Hawker and Buttrose, 1980; Martínez-Gómez et al., 2008; Serrano et al., 2011; Zhu et al., 2017; Guo et al., 2021) Because almond maturation is influenced by the environment (Sakar et al., 2019)(, climate (Oručević and Aliman, 2018; Parker and Abatzoglou, 2018; Díez-Palet et al., 2019), and irrigation strategies (Egea et al., 2009), green almond harvest varies from year to year and orchard to orchard. The aim of this study was to investigate the physical properties of green almonds for use in designing harvesting and sorting machines. Additionally, the mechanical behavior of green almonds under compression at three perpendicular directions and three different speeds was studied to evaluate their mechanical behavior under compression.

2. Materials and Methods

Green almonds of the Sahand variety (Figure 1) were obtained during spring (April) 2021 from a garden in Shiraz, Iran. Sahand almond is a hybrid late-blooming and hard-shelled variety that matures up to the end of summer (September) (Eskandari and Majidazar, 2009). Samples were stored $4\pm1^{\circ}C$ in a refrigerator for 24 hours and brought to room temperature (22˚C) before the experiments. In the laboratory, 50 samples were randomly selected, excluding samples with visible markings. The initial moisture content was obtained by oven drying the green almonds in a laboratory oven at $75\pm0.5^{\circ}C$ for 24 hours (Shirmohammadi et al., 2018). On three replicates, the moisture content was found to be 90% on a wet basis; the initial weight of each replicate before drying was about 40 g. All samples for measuring physical properties were randomly selected. During the experiment, the Laboratory temperature averaged 22 ˚C, with relative humidity ranging from 25 to 30 percent.

Figure 1. A green almond cut in half to view kernel appearance.

2.1. Physical Properties of green almonds

The physical properties of the green almonds were measured in random order. The properties of length (L), width (W), thickness (T), mass (M), and volume (V) were measured for each of the 50 samples. Dimensions were measured using a digital caliper with an accuracy of 0.01 mm (Mitutoyo, Japan), and weight was measured using a digital balance with an accuracy of 0.01 g (A &D FX-3000 GD, Japan). Arithmetic mean diameter (D_a) and geometric mean diameter (D_g) were calculated using Eq. 1 and Eq. 2 respectively (Mohsenin, 1986).

$$D_a = \frac{L + W + T}{3} \quad (1)$$

$$D_g = \sqrt[3]{LWT} \quad (2)$$

Eq. 3 and Eq. 4 were used to calculate the surface area (Sa) (Mohsenin, 1986) and projected area (Pa) (Khazaei et al., 2006) respectively.

$$S_a = \pi {D_g}^2 \quad (3)$$

$$P_a = \frac{\pi LW}{4} \quad (4)$$

Eq. (5) shows the ratio of width to length, which is called the aspect ratio (R_a). Sphericity () in Eq. (6) determines the closeness of the sample's shape to that of a sphere (Mohsenin, 1986). A sphere sample has a sphericity equal to one.

$$R_a = \frac{W}{L} \quad (5)$$

$$\Phi = \frac{\sqrt[3]{LWT}}{L} = \frac{D_g}{L} \quad (6)$$

The theoretical volume of the green almonds (Khazaei et al., 2006; Remón et al., 2021) was calculated using Eq. (7). The results can be compared with the actual volume of each sample as measured with Eq. (8) using the platform method (Mohsenin, 1986). Comparison of the theoretical and the actual volume has been done for other agricultural products as well (Seyedabadi et al., 2011). In this equation, W_T and ρ_T correspond with the weight and density of toluene (C_7H_8), respectively. Compared to water, toluene has a lower surface tension (McLinden and Splett, 2008) which makes it suitable for measuring the volume of textured samples like peach (Emadi et al., 2011). Toluene's density is also lower than water which ensures submergence of the sample (Yan et al., 2008). Therefore, green almond samples were submerged in toluene instead of water due to the texture of the green almonds.

$$V_t = \frac{\pi {D_g}^3}{6} \quad (7)$$

$$V = \frac{W_T}{\rho_T} \quad (8)$$

Bulk density (ρ_b) is defined by the mass of green almonds divided by the volume of the container. In this study, green almonds were poured into a cylinder of known volume and the mass was measured by the digital balance. Bulk density (ρ_b) was used with true density (ρ_t) for calculating porosity (ε) with Eq. (9) (Mohsenin, 1986).

$$\varepsilon = \frac{\rho_t - \rho_b}{\rho_t} \quad (9)$$

The static friction coefficient (μ) of samples was calculated with Eq. (10) (Mohsenin, 1986) on three surfaces of MDF (medium density fiberboard), galvanized iron, and rubber. These materials were chosen for this test because agricultural products come into contact with them during mechanical harvest and they have been used in previous studies (Askari Asli-Ardeh et al., 2017; Jahanbakhshi et al., 2019). Random samples were placed on the surface, and the slope of the surface was increased until the samples started to move down at constant speed. At this point, the angle of the surface with the horizon (α) was recorded, and the tangent of this angle is known as the static friction coefficient (Figure 2). This procedure was repeated ten times for each of the three surfaces.

$$\mu = \tan \alpha \quad (10)$$

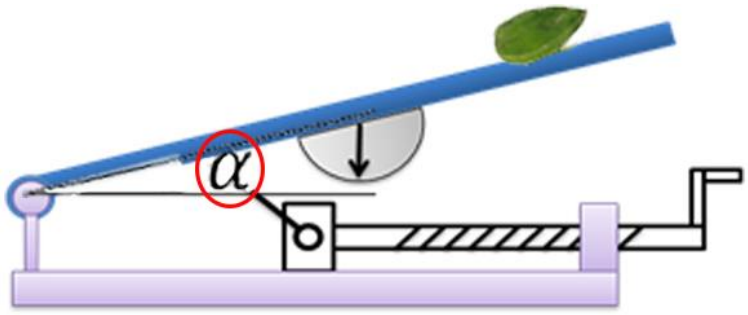

Figure 2. Schematic of slide angle coefficient of friction (COF) Tester.

2.2. Mechanical Behavior of green almonds

The behavior of green almonds under compression was studied using the uniaxial compression test (Tinus Olsen H5KS, England) with a completely randomized factorial experiment in triplicate. The tests (Figure 3) were conducted in three directions (X, Y, and Z), correlating with the sample's three dimensions (length, width, and thickness, respectively) and at three speeds (10, 15, and 20 mm/min) (Mirae et al. 2016). After each test, the rupture force, deformation, and absorbed energy until failure were recorded. A green almond under compression can be seen in Figure 4. Overall, the test was conducted on 27 green almonds.

Minitab (version 17.3.1) was used for statistical analysis of the results. The Pearson correlation method was used to find the correlation between green almond physical properties. General factorial regression was utilized for analyzing the results of compression tests. Means comparisons were made using the Fisher comparison method at specified confidence levels.

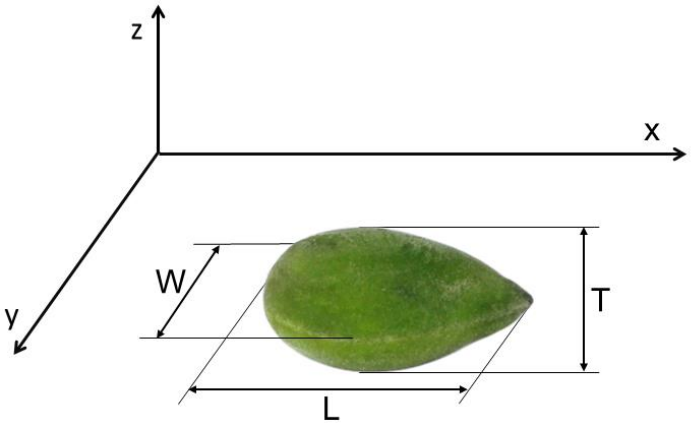

Figure 3. The coordinate system and the green almond's three dimensions.

Figure 4. A green almond under compression test along its length (X direction), SDL Atlas universal testing machine (Tinus Olsen LTD. UK).

3. Results and Discussion

3.1. Physical Properties

A summary of the physical properties of green almonds can be seen in Table 1. The average values for length, width, and thickness of green almonds were 29.73, 20.23, and 15.02 mm, respectively. The arithmetic and geometric mean diameters were 21.66 and 20.81 mm, respectively. The surface area was 1366.77 mm^2, and the projected area was found to be 473.59 mm^2. Additionally, aspect ratio and sphericity were 0.68 and 0.70, respectively. On average, a green almond weighed 4.14 g with a volume of 3.78 cm^3. Finally, the average true density of green almond was 1.10 g/cm^3 and, with a bulk density of 0.62 g/cm^3, green almond porosity was 0.44.

Table 1. Physical properties of green almond

Parameter	Abbreviation	Mean	Min	Max	SD	CV%
Length (mm)	L	29.73	26.72	33.89	1.60	5.37
Width (mm)	W	20.23	16.40	24.44	1.73	8.54
Thickness (mm)	T	15.02	12.36	18.51	1.44	9.57
Arithmetic Mean Diameter (mm)	D_a	21.66	18.96	24.65	1.40	6.46
Geometric Mean Diameter (mm)	D_g	20.81	17.86	24.11	1.46	7.02
Surface Area (mm^2)	S_a	1366.77	1002.46	1826.96	192.56	14.09
Projected Area (mm^2)	P_a	473.59	362.20	600.47	59.88	12.64
Aspect Ratio	R_a	0.68	0.58	0.79	0.05	6.74
Sphericity	Φ	0.70	0.63	0.78	0.03	4.60
Mass (g)	M	4.14	2.84	6.25	0.85	20.57
Theoretical Volume (cm^3)	V_t	4.79	2.99	7.34	1.02	21.23
Volume (cm^3)	V	3.78	2.41	6.17	0.87	22.96
True Density (g/cm^3)	ρ_t	1.10	0.87	1.33	0.07	6.31
Porosity	ε	0.44	0.29	0.53	0.04	8.42

The length and width of green almonds were about 83% of that of mature almonds, and the green almonds' thickness was 90% of that of mature almonds of the same variety without the green hull (Rasouli et al., 2010). The sphericity and mass of mature almonds of Sahand variety were found to be

0.67 and 4.18 g, respectively (Rasouli et al., 2010), which are very close to that of the green almonds in this study. Another study (Murathan et al., 2020) has also measured the weight of green almonds. However, due to the differences between varieties, the samples' weights are more than twice the average weight measured in this study.

A correlation between most of the physical parameters using the Pearson method can be seen in Table 2. All of the parameters shown in this table are highly correlated except for green almonds' true density, which is only correlated to volume. Length and sphericity are also not correlated.

Table 2. Pearson correlation coefficients for physical properties of green almond

	L	W	T	D_a	D_g	S_a	Φ	M	P_a	V
W	0.615**									
T	0.548**	0.831**								
D_a	0.821**	0.930**	0.892**							
D_g	0.753**	0.941**	0.934**	0.993**						
S_a	0.755**	0.939**	0.933**	0.993**	0.999**					
Φ	-0.014	0.720**	0.781**	0.558**	0.647**	0.641**				
M	0.743**	0.904**	0.857**	0.948**	0.947**	0.947**	0.577**			
P_a	0.847**	0.939**	0.797**	0.981**	0.960**	0.961**	0.478**	0.930**		
V	0.720**	0.863**	0.830**	0.913**	0.912**	0.913**	0.552**	0.959**	0.893**	
ρ_t	-0.162	-0.192	-0.222	-0.217	-0.221	-0.219	-0.153	-0.202	-0.201	-0.464**

**Significant at 0.01 probability level

Theoretical volume is significantly (1% confidence level) larger than the actual volume of the green almonds, and therefore, Eq. (7) does not accurately represent the volume of green almonds.

Based on the Pearson correlation coefficients in Table 2, the volume of green almond is correlated with its three dimensions and mass. A model for volume based on the three dimensions is shown in Eq. (11). Additionally, using Eq. (12), volume can be modelled using mass with an R^2 greater than 90%. Linear model of volume based on mass is shown in Figure 5.

$$V = -8.023 + 0.1549L + 0.2071W + 0.2006T,\ R^2 = 83.58\% \quad (11)$$

$$V = -0.2650 + 0.9768M,\ R^2 = 91.9\% \quad (12)$$

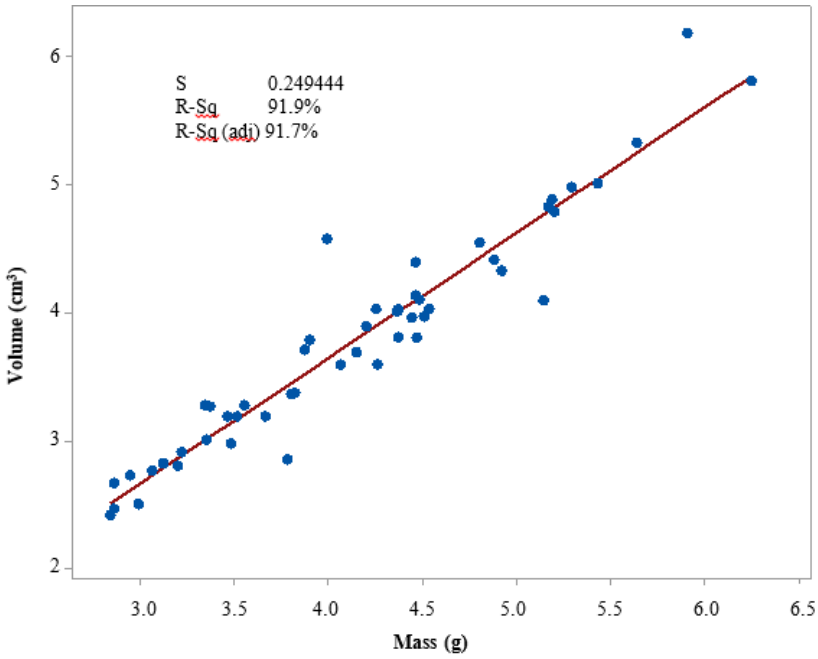

Figure 5. Linear model for green almond's volume based on mass

Green almond mass can be modelled based on its dimensions. Using only one dimension, width can give the most accurate model with an R^2 of 81.72%, as shown in Eq. (13) and Figure 6. The linear model for mass based on the green almond's dimensions in Eq. (14) has an R^2 of around 90%.

$$M = -4.883 + 0.4462W,\ R^2 = 81.72\% \quad (13)$$

$$M = -7.818 + 0.1507L + 0.2336W + 0.1835T,\ R^2 = 90.28\% \quad (14)$$

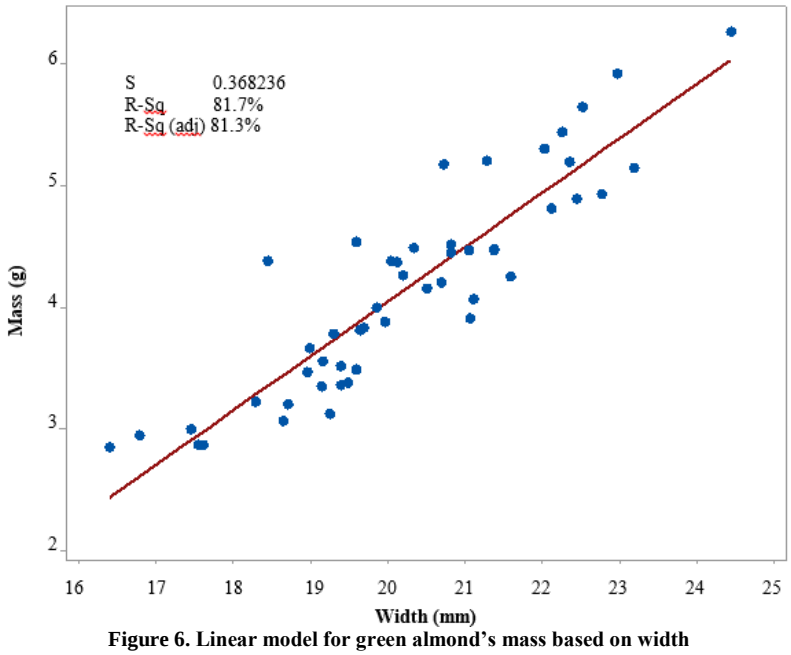

Figure 6. Linear model for green almond's mass based on width

The static friction coefficient of green almonds on three surfaces is presented in Table 3. Different letters within a column represent statistically significant differences by Fisher's test at 1% confidence level. The static friction coefficient of green almonds on MDF and rubber is not significantly different at 0.519 and 0.523, respectively. The static friction coefficient of green almonds on galvanized iron is significantly lower than that of MDF and rubber. This coefficient is essential for the design of harvest, transport, and storage equipment.

Table 3. Static friction coefficient of green almond

Surface Type	Mean	Min	Max	SD	CV%
MDF	0.519[a]	0.488	0.554	0.025	4.88
Galvanized Iron	0.441[b]	0.424	0.466	0.017	3.96
Rubber	0.523[a]	0.488	0.577	0.034	6.51

Table 4. Analysis of variance for the mechanical properties of green almond in compression test.

Source	DF	Seq SS	Contribution	Adj SS	Adj MS	F-Value	P-Value
Model	8	61.246	61.20%	61.246	7.6557	3.55	0.012**
Linear	4	52.403	52.36%	52.403	13.1008	6.07	0.003**
Direction	2	51.164	51.12%	51.164	25.5818	11.86	0.001**
Speed	2	1.240	1.24%	1.240	0.6198	0.29	0.754ns
2-Way Interactions	4	8.843	8.84%	8.843	2.2107	1.02	0.421ns
Direction*Speed	4	8.843	8.84%	8.843	2.2107	1.02	0.421ns
Error	18	38.830	38.80%	38.830	2.1572		
Total	26	100.076	100.00%				

3.2. Mechanical Behavior

As explained in the materials and methods section, the mechanical behavior of green almonds was studied using two factors: compression direction and compression speed. While the direction of compression significantly affected the results (confidence level of 1%), for the speed range investigated in this experiment (10 to 20 mm/min), speed had no significant effect on the results (confidence level of 1%) (Table 4). A study conducted on the mechanical behavior of mature almonds under compression found that both compression direction and speed significantly affect the rupture force of almonds with a confidence level of 1% (Altuntas et al., 2010). Therefore, the mechanical properties of green almonds are only grouped according to compression direction in Table 5. This table shows that the greatest rapture force was observed in the Z direction, while the most energy was absorbed in the X direction. Using the Fisher comparison method, the mean of deformation in the X direction is significantly higher than the means in the other two directions at a 5% confidence level. Figure 7 presents a slight but insignificant (1% and 5% confidence levels) increase in deformation before rupture with increased compression speed from 10 to 15 mm/min, which then drops to around 5 mm at 20 mm/min. Furthermore, deformation decreases significantly from 7.317 mm in the X direction to 5.390 and 3.957 mm in the Y and Z directions. The combined effect of speed and direction on deformation can be seen in Figure 7.

Table 5. Mechanical properties of green almond.

Parameter	Direction	Mean	Min	Max	SD
Rupture Force (N)	X	70.96	45.50	104.00	18.91
	Y	67.18	43.50	120.10	23.50
	Z	86.63	44.85	146.90	34.31
Deformation (mm)	X	7.317	4.913	9.730	1.344
	Y	5.390	3.825	9.070	1.603
	Z	3.957	2.560	6.920	1.318
Absorbed Energy (J)	X	0.3366	0.1755	0.9810	0.2600
	Y	0.1691	0.0578	0.4360	0.1115
	Z	0.1289	0.0482	0.2786	0.0779

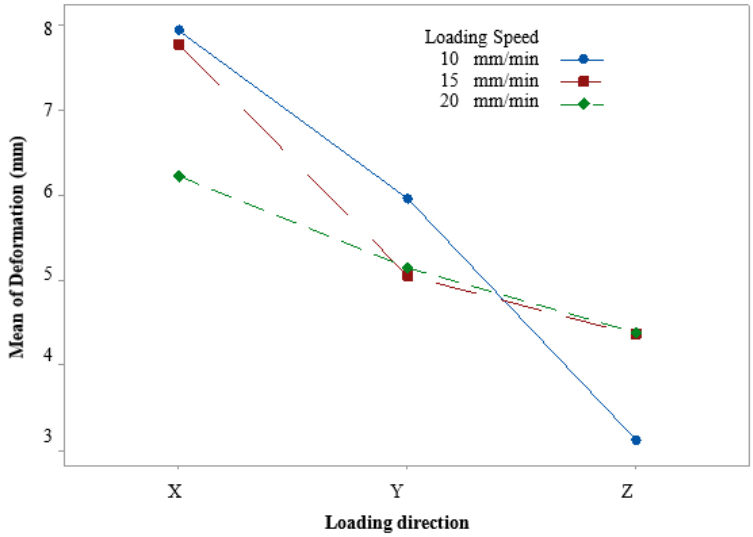

Figure 7. Interaction plot showing the effect of direction and speed on green almond deformation.

4. Conclusion

This study evaluated the physical properties of the Sahand variety of green almond and its behavior under compression at different directions and speeds. It was found that, because of its shape, the theoretical equation for volume could not accurately represent green almond volume, and a new model for calculating the volume was proposed. The static friction coefficient of green almonds on MDF and rubber is greater than that on galvanized iron. The results of the uniaxial compression test suggest that compression speed does not significantly affect the mechanical behavior of green almonds and that they can endure the most deformation along the X direction (length). These findings may be used to facilitate studies and further developments in mechanical harvesting and post-harvesting of green almonds.

Declarations

Funding and competing interests

The authors have no relevant financial or non-financial interests to disclose.

CRediT authorship contribution statement

Jalal Baradaran Motie: Methodology, Validation, Formal analysis, Investigation, Resources, Writing - Reviewing and Editing, Supervision. **Hajarsadat S Lavasani:** Conceptualization, Formal analysis, Investigation, Resources, Writing - Original Draft, Visualization.

Acknowledgements

The authors would like to thank the almond producer for providing the green almonds.

References

Ahmadpour, A., Tahmasbi, M., Bastami, T.R., Besharati, J.A., 2009. Rapid removal of cobalt ion from aqueous solutions by almond green hull. Journal of Hazardous Materials 166, 925-930.

Aktas, T., Polat, R., Atay, U., 2007. Comparison of mechanical properties of some selected almond cultivars with hard and soft shell under compression loading. Journal of Food Process Engineering 30, 773-789.

Akubude, V.C., Nwaigwe, K.N., 2016. Economic importance of edible and non-edible almond fruit as bioenergy material: a review. American Journal of Energy Science 3, 31-39.

Altuntas, E., Gercekcioglu, R., Kaya, C., 2010. Selected mechanical and geometric properties of different almond cultivars. International Journal of Food Properties 13, 282-293.

Appah, S., Wang, P., Ou, M., Gong, C., Jia, W., 2019. Review of electrostatic system parameters, charged droplets characteristics and substrate impact behavior from pesticides spraying. International Journal of Agricultural and Biological Engineering 12, 1-9.

Askari Asli-Ardeh, E.A., Mohammad Zadeh, H., Abbaspour-Gilandeh, Y., 2017. Determination of dynamic friction coefficient in common wheat varieties on different contact surfaces. Agricultural Engineering International: CIGR Journal 19, 136-141.

Aydin, C., 2003. Physical properties of almond nut and kernel. Journal of food engineering 60, 315-320.

Baradaran Motie, J., Miraei Ashtiani, S.H., Abbaspour-Fard, M.H., Emadi, B., 2014. Modeling physical properties of lemon fruits for separation and classification. International Food Research Journal 21, 1901-1909.

Demir, B., Sayinci, B., Çetin, N., Yaman, M., Çömlek, R., 2019. Shape discrimination of almond cultivars by Elliptic Fourier Descriptors. Erwerbs-Obstbau 61, 245-256.

DePeters, E., Swanson, K., Bill, H., Asmus, J., Heguy, J., 2020. Nutritional composition of almond hulls. Applied Animal Science 36, 761-770.

Díez-Palet, I., Funes, I., Savé, R., Biel, C., de Herralde, F., Miarnau, X., Vargas, F., Àvila, G., Carbó, J., Aranda, X., 2019. Blooming under Mediterranean climate: Estimating cultivar-specific chill and heat requirements of almond and apple trees using a statistical approach. Agronomy 9, 760.

Egea, G., González-Real, M.M., Baille, A., Nortes, P.A., Sánchez-Bel, P., Domingo, R., 2009. The effects of contrasted deficit irrigation strategies on the fruit growth and kernel quality of mature almond trees. Agricultural water management 96, 1605-1614.

Emadi, B., Abolghasemi, R., Aghkhani, M.H., Beyraghi Toosi, S., 2011. Physical and mechanical properties of peach. World Applied Sciences Journal 12, 119-122.

Esfahlan, A.J., Jamei, R., Esfahlan, R.J., 2010. The importance of almond (*Prunus amygdalus* L.) and its by-products. Food chemistry 120, 349-360.

Eskandari, S., Majidazar, M., 2009. Introduction of new hybrid varieties of almond (*Prunus amygdalus* Batsch) for almond producing regions of Iran. World Applied Sciences Journal 6, 323-330.

Eski, İ., Demir, B., Gürbüz, F., Kuş, Z.A., Yilmaz, K.U., Uzun, M., Ercişli, S., 2018. Design of neural network predictor for the physical properties of almond nuts. Erwerbs-Obstbau 60, 153-160.

Essabir, H., Nekhlaoui, S., Malha, M., Bensalah, M., Arrakhiz, F., Qaiss, A., Bouhfid, R., 2013. Bio-composites based on polypropylene reinforced with Almond Shells particles: Mechanical and thermal properties. Materials & Design 51, 225-230.

FAOSTAT, 2021. FAO Global Statistical Yearbook. FAO, Rome.

Ferrandez-Villena, M., Ferrandez-Garcia, C.E., Garcia Ortuño, T., Ferrandez-Garcia, A., Ferrandez-Garcia, M.T., 2019. Study of the utilisation of almond residues for low-cost panels. Agronomy 9, 811-820.

Gradziel, T.M., 2020. Redomesticating almond to meet emerging food safety needs. Frontiers in Plant Science 11, 778.

Guo, C., Wei, Y., Yang, B., Ayup, M., Li, N., Liu, J., Liao, K., Wang, H., 2021. Developmental transcriptome profiling uncovered carbon signaling genes associated with almond fruit drop. Scientific reports 11, 3401.

Gupta, A., Sharma, R., Sharma, S., 2020. Almond. In: Nayik, G.A., Gull, A. (Eds.), Antioxidants in Vegetables and Nuts-Properties and Health Benefits. Springer, Singapore, pp. 423-452.

Hawker, J., Buttrose, M., 1980. Development of the almond nut (*Prunus dulcis* (Mill.) DA Webb). Anatomy and chemical composition of fruit parts from anthesis to maturity. Annals of Botany 46, 313-321.

Huang, G., Lapsley, K., 2019. Almonds. In: Pan, Z., Zhang, R., Zicari, S. (Eds.), Integrated Processing Technologies for Food and Agricultural By-Products. Academic Press, pp. 373-390.

Jahanbakhshi, A., Rasooli Sharabiani, V., Heidarbeigi, K., Kaveh, M., Taghinezhad, E., 2019. Evaluation of engineering properties for waste control of tomato during harvesting and postharvesting. Food science & nutrition 7, 1473-1481.

Khazaei, J., Sarmadi, M., Behzad, J., 2006. Physical properties of sunflower seeds and kernels related to harvesting and dehulling. Lucrari Stiintifice 49, 262-271.

Ledbetter, C.A., Palmquist, D.E., 2006. Comparing physical measures and mechanical cracking products of 'Nonpareil'almond (*Prunus dulcis* [Mill.] DA Webb.) with two advanced breeding selections. Journal of food engineering 76, 232-237.

Liminana, P., Garcia-Sanoguera, D., Quiles-Carrillo, L., Balart, R., Montanes, N., 2018. Development and characterization of environmentally friendly composites from poly (butylene succinate)(PBS) and almond shell flour with different compatibilizers. Composites Part B: Engineering 144, 153-162.

Maniscalco, M., Corrado, C., Volpe, R., Messineo, A., 2020. Evaluation of the optimal activation parameters for almond shell bio-char production for capacitive deionization. Bioresource Technology Reports 11, 100435.

Martínez-Gómez, P., Sánchez-Pérez, R., Dicenta, F., 2008. Fruit development in almond for fresh consumption. Journal-American Pomological Society 62, 82-86.

McLinden, M.O., Splett, J.D., 2008. A liquid density standard over wide ranges of temperature and pressure based on toluene. Journal of Research of the National Institute of Standards and Technology 113.

Miraei Ashtiani, S.H., Rohani, A., Aghkhani, M.H., 2020. Soft computing-based method for estimation of almond kernel mass from its shell features. Scientia Horticulturae 262, 109071.

Mohsenin, N.N., 1986. Physical Properties of Plant and Animal Materials. Gordon and Breach Science Publishers, New York.

Murathan, Z.T., Kaya, A., Erbil, N., Arslan, M., Dıraz, E., Karaman, Ş., 2020. Comparison of bioactive components, antimicrobial and antimutagenic features of organically and conventionally grown almond hulls. Erwerbs-Obstbau 62, 463-472.

Nasseh, N., Taghavi, L., Barikbin, B., Khodadadi, M., 2017. Advantage of almond green hull over its resultant ash for chromium (VI) removal from aqueous solutions. International Journal of Environmental Science and Technology 14, 251-262.

Oručević, A., Aliman, J., 2018. The phenology of flowering and ripening of almond cultivars Nonpareil, Texas, Ferraduel and Genco in Herzegovina. International Journal of Plant & Soil Science 21, 1-9.

Özcan, M.M., Ünver, A., Erkan, E., Arslan, D., 2011. Characteristics of some almond kernel and oils. Scientia Horticulturae 127, 330-333.

Parker, L.E., Abatzoglou, J.T., 2018. Shifts in the thermal niche of almond under climate change. Climatic change 147, 211-224.

Pirayesh, H., Khazaeian, A., 2012. Using almond (*Prunus amygdalus* L.) shell as a bio-waste resource in wood based composite. Composites Part B: Engineering 43, 1475-1479.

Prgomet, I., Gonçalves, B., Domínguez-Perles, R., Pascual-Seva, N., Barros, A.I., 2017. Valorization challenges to almond residues: Phytochemical composition and functional application. Molecules 22, 1774.

Rasouli, M., Mollazade, K., Fatahi, R., Zamani, Z., Imani, A., Martínez-Gómez, P., 2010. Evaluation of Engineering Properties in Almond Nuts. International Journal of Natural & Engineering Sciences 4, 17-26.

Remón, J., Latorre-Viu, J., Matharu, A.S., Pinilla, J.L., Suelves, I., 2021. Analysis and optimisation of a novel 'almond-refinery'concept: Simultaneous production of biofuels and value-added chemicals by hydrothermal treatment of almond hulls. Science of The Total Environment 765, 142671.

Sakar, E.H., El Yamani, M., Rharrabti, Y., 2019. Geometrical Traits in Almond Fruit as Affected by Genotypic and Environmental Variations in Northern Morocco. Erwerbs-Obstbau 61, 103-112.

Serrano, N., Lovera, M., Salguero, A., Arquero, O., Casado, B., Fernández, J., 2011. Flowering and maturation dates of the main late-blooming almond varieties of the Mediterranean basin. Acta horticulturae, 99-102.

Seyedabadi, E., Khojastehpour, M., Sadrnia, H., Saiedirad, M.-H., 2011. Mass modeling of cantaloupe based on geometric attributes: A case study for Tile Magasi and Tile Shahri. Scientia Horticulturae 130, 54-59.

Shirmohammadi, M., Charrault, E., Blencowe, A., 2018. Micromechanical properties of almond kernels with various moisture content levels. International Journal of Food Properties 21, 1820-1832.

Yan, Z., Sousa-Gallagher, M.J., Oliveira, F.A.R., 2008. Shrinkage and porosity of banana, pineapple and mango slices during air-drying. Journal of Food Engineering 84, 430-440.

Zahedi, S.M., Abdelrahman, M., Hosseini, M.S., Yousefi, R., Tran, L.-S.P., 2020. Physical and biochemical properties of 10 wild almond (Amygdalus scoparia) accessions naturally grown in Iran. Food Bioscience 37, 100721.

Zhu, Y., Wilkinson, K.L., Wirthensohn, M., 2017. Changes in fatty acid and tocopherol content during almond (*Prunus dulcis*, cv. Nonpareil) kernel development. Scientia Horticulturae 225, 150-155.